Microphase Separation and Shear Alignment of Gradient Copolymers: Melt Rheology and Small-Angle X-Ray Scattering Analysis

Michelle M. Mok,[†] Saswati Pujari,[‡] Wesley R. Burghardt,[†,‡] Christine M. Dettmer,[§] SonBinh T. Nguyen,[§] Christopher J. Ellison,[||] and John M. Torkelson*[,†,‡]

Department of Materials Science and Engineering, Department of Chemical and Biological Engineering, and Department of Chemistry, Northwestern University, Evanston, Illinois 60208, and Department of Chemical Engineering and Materials Science, University of Minnesota, Minneapolis, Minnesota 55455

Received April 27, 2008

ABSTRACT: The degree of microphase or nanophase segregation in gradient copolymers with compositions varying across the whole copolymer backbone is studied via low-amplitude oscillatory shear (LAOS) measurements and small-angle X-ray scattering (SAXS). Studies are done as a function of comonomer segregation strength, molecular weight (MW), gradient architecture and temperature. Controlled radical polymerization is used to synthesize strongly segregating styrene/4-acetoxystyrene (S/AS) and the more weakly segregating S/*n*-butyl acrylate (S/nBA) gradient copolymers. Results are compared to those from S/AS and S/nBA random and block copolymers. The higher MW S/AS gradient copolymer exhibits LAOS behavior similar to the highly microphase segregated S/AS block copolymer, while the lower MW S/AS gradient copolymer exhibits complex, nonterminal behavior indicative of a lower degree of microphase segregation. The S/nBA gradient copolymers demonstrate more liquidlike behavior, with the lower MW sample exhibiting near-Newtonian behavior, indicative of a weakly segregating structure, while the higher MW, steeper gradient sample shows behavior ranging from solidlike to more liquidlike with increasing temperature. With the exception of the lower MW S/nBA case, the gradient copolymers exhibit temperature-dependent LAOS behavior over a wide temperature range, reflecting their temperature-dependent nanodomain composition amplitudes. The S/AS samples have SAXS results consistent with the degree of microphase segregation observed via rheology. Shear alignment studies are done on the higher MW S/AS gradient copolymer, which is the most highly microphase segregated gradient copolymer. Rheology and SAXS provide evidence of shear alignment, despite the gradual variation in composition profile across the nanodomains of such gradient copolymers. A short review of the nomenclature and behavior of linear copolymer architectures is also provided.

Introduction

A/B block copolymers order into phase-segregated, nanostructured materials under appropriate conditions while A/B random copolymers are homogeneous under all conditions.[1–3] A subclass of copolymer that can also yield phase-segregated nanostructures consists of chains containing one block of A units (or nearly pure A units), a second block tapering from nearly pure A to nearly pure B units, and often (but not always) a third block of pure B units (or nearly pure B units); such copolymers were coined "tapered block copolymers" 30−40 years ago[4–9] and are sometimes also referred to as "graded block copolymers".[10–12] (For an overview distinguishing among the different types of linear copolymers discussed in the research literature and the associated, overlapping copolymer terminology, please refer to the section entitled Nomenclature and Behavior Associated with Linear Copolymers.) Scattering, rheology and electron microscopy have provided direct evidence of ordered block and tapered block copolymers, both in the absence and presence of external fields yielding alignment.[7,11,13–24] Here, we consider the ordering, phase behavior and shear-flow alignment of a linear copolymer chain differing from block, tapered block, and random copolymers—the gradient copolymer with a composition gradient along the whole copolymer chain backbone.[25,26] This sequence distribution along the gradient copolymer backbone reduces the interchain and intrachain repulsion compared to block copolymers but does not distribute it uniformly, as in random copolymers.[25,27–29] Because of the gradual change in composition along their chain length, such gradient copolymers have advantages in applications ranging from use as compatibilizers of immiscible blends[30–32] and stabilizers for emulsion polymerization[33] to vibration/acoustic damping materials.[34] Simulations and theoretical modeling have predicted that neat gradient copolymers can segregate into lamellar, hexagonal, body-centered cubic and double-gyroid nanostructures.[25,35]

While these nanostructures are analogous to those in block copolymers, major differences in composition profiles are expected between domains of segregated A/B gradient copolymers with composition gradients along the whole copolymer backbone and domains of segregated A/B block copolymers. Using self-consistent field theory, Lefebvre et al.[36] predicted that microphase or nanophase separated symmetric A/B gradient copolymers have sinusoidal composition profiles across lamellae, even in the strong segregation regime, instead of the steplike profiles obtained with A/B block copolymers. This implies that a wide range of local compositions are present (although not pure A or B) in segregated gradient copolymers that possess a composition gradient along their whole chain length, yielding materials that may be described as totally interphase[7,34] with no well-defined nanodomain boundaries. This is different from segregated block copolymers where pure-A and pure-B nanodomains are separated by interfaces several nanometers in width. Their unique combination of composition profiles and

* To whom correspondence should be addressed. E-mail: j-torkelson@northwestern.edu.
[†] Department of Materials Science and Engineering, Northwestern University.
[‡] Department of Chemical and Biological Engineering, Northwestern University.
[§] Department of Chemistry, Northwestern University.
[||] Department of Chemical Engineering and Materials Science, University of Minnesota.

10.1021/ma8009454 CCC: $40.75
Published on Web 07/02/2008

morphology in the segregated state raises questions regarding the extent to which gradient copolymers with composition gradients along the whole copolymer backbone will exhibit the signatures of block copolymer microphase segregation such as long-range ordering and shear alignment.

Lefebvre et al.[36] also predicted that the critical value of χN for microphase segregation, $(\chi N)_c$, is higher for such gradient copolymers than for block copolymers ($(\chi N)_c = 29.25$ for a copolymer with a linear composition gradient across the whole chain compared to 10.5 for a block copolymer) and that the A-rich and B-rich regions of gradient copolymers grow richer in A and B with respect to χN much more slowly than block copolymers. (χ is the Flory−Huggins interaction parameter, and N is the effective number of copolymer repeat units.) The latter prediction suggests that such gradient copolymers can be designed to undergo transitions from microphase separation to fully homogeneous behavior over much broader temperature ranges than block copolymers. The larger temperature range associated with gradient copolymer microphase separation relative to that associated with block copolymer microphase separation is likely to be further broadened by the greater degree of heterogeneity in chain structure (local sequence distribution within the chain *and* overall number of repeat units) of gradient copolymers relative to block copolymers. For a given block copolymer system, the spectrum of behavior ranging from homogeneous to microphase separated can be observed at experimentally feasible temperatures only for narrow ranges of molecular weight with χN values close to $(\chi N)_c$.[37–39] By manipulating the gradient profile, this behavior may potentially be seen at much higher molecular weights in gradient copolymers than for block copolymers.

Most of the current experimental support for microphase segregation of gradient copolymers with composition gradients across much or all of the chain length is indirect, coming from glass transition temperature (T_g) studies that indicate the range of local compositions present.[31,40–47] Differential scanning calorimetry (DSC) of gradient copolymers has revealed a single, broad glass transition region (~80 °C or greater in breadth in some cases),[31,45,47] in contrast to the single, narrow T_g observed in random copolymers and the two distinct, narrow T_gs typically observed in segregated block copolymers. The broad glass transition range present in some gradient copolymers can span much of the range intermediate to the corresponding homopolymer T_gs, and the breadth may be tuned by the strength of the composition gradient and comonomer selection. These results are consistent with the prediction by Lefebvre et al.[36] of sinusoidal composition profiles within lamellar gradient copolymer nanodomains.

Dynamic mechanical analysis (DMA) has also been used to assess the glass transition behavior of gradient copolymers with composition gradients along the whole copolymer backbone.[27,34,42,43] Not only are broad T_gs for such copolymers observed using DMA, but we have also shown[34] that the shapes of the curves expressing the temperature dependence of E' and E'' (the storage tensile modulus and loss tensile modulus, respectively) correspond very well to results modeled 25 years ago by Hashimoto et al.[7] for a hypothetical segregated copolymer with a perfectly sinusoidal composition profile across lamellar nanodomains. Hashimoto et al.[7] described their hypothetical system as consisting of all interphase, with no single-composition domains. They also did experiments[7] to evaluate the DMA behavior of tapered block copolymers synthesized in their group or received from Phillips Petroleum Co.[48–50] However, none of the many experimental systems they studied exhibited behavior similar to that we have recently observed[34] in gradient copolymers with a composition gradient along the whole copolymer chain. Instead, the copolymers studied by Hashimoto et al. exhibited behavior that they described as "enhancement of mixing of unlike segments in the interfacial region... between two coexisting microphases... designated as domain−boundary effect"[7] and "enhancement of mixing of unlike segments in the domains... designated as mixing-in-domain effect."[7]

Direct structural evidence of phase segregation in neat gradient copolymers with full composition gradients across the chain length is severely limited.[51] No report of nanostructured gradient copolymers has been made via electron microscopy, which is likely due to the inherently low contrast relative to block copolymers, since there is an absence of distinct, pure domains and boundaries in such gradient copolymer systems. However, reports of phase segregated gradient copolymers have been made using atomic force microscopy (AFM).[42,43,52] In 2006, Karaky et al.[42] reported via AFM the presence of randomly ordered harder "spots" (with an apparent size scale of order 10 nm or a few tens of nanometers) on a styrene/butyl acrylate gradient copolymer surface after it had been rasped; these regions were attributed to aggregated styrene-rich domains. A 2007 study[43] compared the AFM characterization of the surface morphologies of gradient and block copolymers of dimethylacrylamide and butyl acrylate, with a reported radius of the apparent surface lamella of 750 nm for a gradient copolymer. (Although not explained in this manner in ref 43, such results may be consistent with the presence of a segregated gradient copolymer morphology with associated hole or island formation and growth on the top surface of the film, similar to that observed in some thin block copolymer films.[53])

Scattering and melt rheology studies of phase segregation in neat gradient copolymers with full composition gradients across the copolymer chain are also very limited. Karaky et al.[42] performed small-angle neutron scattering on a styrene/butyl acrylate gradient copolymer and reported a single scattering peak corresponding to an average distance between domains of 28.6 nm. The only reported study on the temperature-dependent phase behavior of gradient copolymers was conducted by Matyjaszewski et al.,[27] who used a combination of low amplitude oscillatory shear measurements and small-angle X-ray scattering (SAXS) to characterize two molecular weights of styrene/acrylonitrile gradient copolymers. With increasing melt-state temperature, the lower molecular weight copolymer showed flow regime behavior and a gradual disappearance of its scattering peak while the higher molecular weight sample exhibited a solidlike plateau in storage modulus and only a slight reduction of its SAXS peak.[27]

Here, we examine gradient copolymers where the gradient dominates in the copolymer architecture resulting in nanophase separated systems with no single-composition domains, i.e., the copolymer system described by Hashimoto et al.[7] as consisting of interphase. These materials were synthesized via nitroxide-mediated controlled radical polymerization,[54,55] which allows for both a simpler synthesis method and more direct control over gradient structures than the anionic polymerization methods often used to create tapered block copolymers. Using melt rheology and SAXS, we provide experimental evidence of microphase segregation, temperature-dependent phase behavior and, for the first time, shear alignment in gradient copolymers. Specifically, we investigate styrene/4-acetoxystyrene (S/AS) and styrene/*n*-butyl acrylate (S/nBA) gradient copolymers using low amplitude oscillatory shear measurements, high amplitude oscillatory shear alignment, solid-state SAXS, and SAXS during steady shear.

Nomenclature and Behavior Associated with Linear Copolymers. In this section, we distinguish among many of the linear copolymer types named in the research literature. Depictions of these copolymers are shown in Figure 1, after

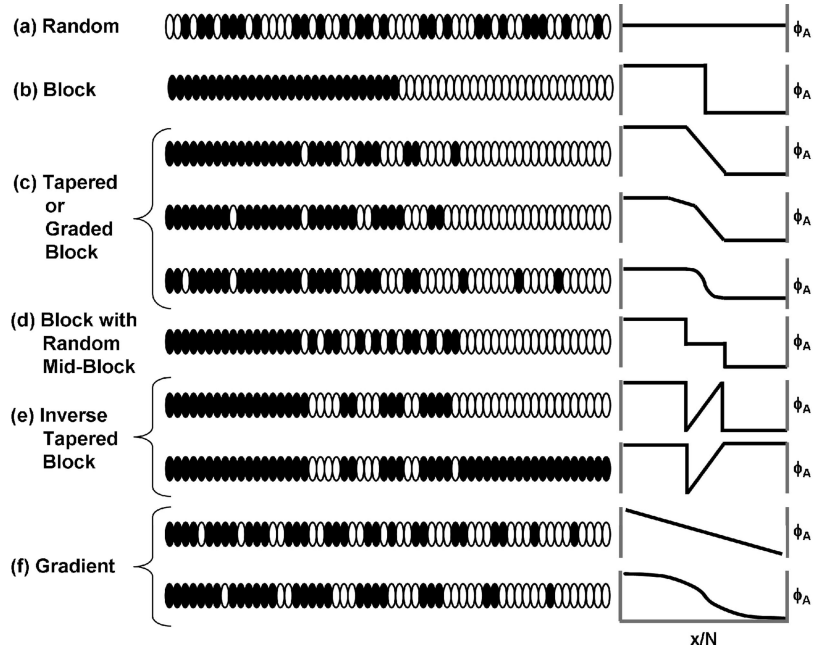

Figure 1. Schematics of various linear copolymer structures: (a) random copolymer; (b) block copolymer; (c) tapered or graded block copolymers after ref 57 (top), ref 11 (middle) and ref 25 (bottom); (d) block copolymer with random middle blocks; (e) inverse tapered block copolymers after ref 57 (top) and ref 67 (bottom); (f) gradient copolymers after ref 25 (top) and ref 36 (top and bottom). Blocky gradient copolymers with one homopolymer end block resemble schematic c, top, with one end block missing.

schematics in the literature as well as interpretation of literature descriptions. In each case, a monomer-by-monomer depiction is shown for a shortened chain, and a graphical representation of the monomer composition variation in each depiction is provided at the side. The two classic cases, random copolymers (Figure 1a) and block copolymers (Figure 1b), are also shown.

As mentioned in the Introduction, a subclass of linear copolymers is the "tapered block copolymer"[4–9] or "graded block copolymer".[10–12] The description used in the Introduction—a structure consisting of a block of pure or nearly pure A followed by a block which tapers from nearly pure A to nearly pure B, sometimes having a third pure or nearly pure B block - is widely found in the literature and reflects descriptions of experimental syntheses[5–9,11,12,48,49,56,57] as well as schematic drawings (Figure 1c).[11,25,57] The majority of these materials were prepared prior to the advent of controlled radical polymerization, usually employing anionic polymerization of styrene and diene species,[4–8,11,12,48,49,56–58] with very limited examples involving anionic copolymerization of other comonomer systems.[9] The addition of "randomizers"[7] or "polar modifiers"[59] can help to control the reactivity ratios and promote anionic copolymerization of the styrene and diene species, but usually a styrene-rich block and/or a diene-rich block accompanies the tapered region to yield a A/A → B/B or A/A → B structure. These end blocks provide strong impetus for microphase segregation and typically dominate the material properties, as shown by Hashimoto et al.[7] in a comparison of various tapered block copolymers.[50]

The term "tapered block copolymer" has sometimes been applied to a related class of polymers where there is no actual tapering region;[7] in these cases, pure A and B blocks are separated by a random middle block (A/A-*rand*-B/B) as depicted in Figure 1d.[60–63] Such copolymers have also been called "extended block copolymers"[63] and "triblock copolymers with a random middle block".[62] They have been typically synthesized via sequential anionic polymerization of each block, where the random middle block is created using a mixture of styrene, diene and randomizer. While the random middle block can act to promote mixing of the different end blocks, the material behavior remains end-block-dominated.

"Inverse tapers" have also been incorporated between pure end blocks of different types or pure end blocks of the same type (A/B → A/B or A/B → A/A), as depicted schematically in Figure 1e.[57,64–67] These architectures lead to pure A regions covalently bonded to B-rich regions. Such structures are synthesized using semibatch methods by injection of a styrene/diene monomer mixture into a reactor following the formation of the first homopolymer block; the difference in reactivity ratios creates the taper. These structures facilitate the "mixing-in-domain" effect described by Hashimoto et al.[7] when compared to ABA and AB block copolymers.

Tapered block copolymers and their variants have been widely studied via DMA, SAXS and microscopy. Dynamic mechanical analysis has revealed that the transitional region increases the miscibility of the end blocks, leading to T_g regions shifting and widening.[6–8,48–50,60,64,66,67] As determined by Hashimoto et al.[7] in a study of a variety of tapered block copolymers, the broadened T_gs observed in these materials are attributed to some combination of greater mixing of unlike segments in the domains or in the domain boundaries. In the former case, the T_gs of the two microphases are observed to shift closer together, creating an effectively "broad" T_g when they overlap; typically, the peaks from the two microphases are distinct, unless the composition variation becomes small. In the latter case, there is an increasing contribution from regions intermediate to the homopolymer T_gs; however, due to the end block(s) in the tapered block copolymers, the peaks from the single-phase domains remain visible and dominant. Ordered domains are seen via force and electron microscopy in tapered block copolymers, but with more diffuse boundaries or lower contrast than in block copolymers.[6–8,60,65–67] Reduced SAXS scattering and loss of higher order SAXS peaks are observed in some tapered cases compared to regular block copolymers.[6–8,57,67] Limited temperature-dependent rheological[57,64] and SAXS[6,8] studies have examined the melt-state phase segregation of such materials. Overall, the behavior of these materials indicates that the transitional regions have a compatibilizing effect on the end blocks but that the end block

properties—and corresponding potential for essentially pure microdomains—still dominate in the final product.

The term gradient copolymer was first used in the refereed literature by Pakula and Matyjaszewski in 1996[25,26] to describe a class of copolymers different from block, random, and tapered copolymers. In that theoretical paper, a gradient copolymer was schematically depicted as a linear chain with a continuously varying comonomer composition across the entire chain length (Figure 1f, top), whereas a tapered block copolymer was depicted as having a tapered portion between single-component end blocks (Figure 1c, bottom). This 1996 publication closely followed the first reported synthesis of gradient copolymers by controlled radical polymerization.[68] Since then, many groups[25–36,40–47,55,69–76] have used the term gradient copolymer to refer to copolymers possessing a composition gradient along all or most of the chain length, and this is the definition of gradient copolymer which will be used in the remainder of this text. Gradient copolymers have been synthesized by various controlled radical polymerization (CRP) methods,[28] as well as ring-opening metathesis[69] and cationic[70,71] polymerizations. Researchers have also used CRP to yield structures with single homopolymer end blocks somewhat akin to tapered copolymers; these have typically been designated "blocky gradient copolymers"[44,77–79] in order to distinguish them from purely gradient structures.

There are limited cases from anionic syntheses where copolymers with moderate levels of tapering were created without end blocks;[48,49] the authors referred to these as nonuniformly "random copolymers". The relevant sample in ref 48 exhibits a glass transition region only slightly broadened from the uniformly random case, and the DMA data exhibit a single, dominant peak with a small shoulder. The cumulative styrene composition for such samples in ref 49 varied 10−18% over the extent of the reaction. The viscoelastic responses for these samples were very similar to the uniformly random case, presumably due to the low degree of composition variation; however, there was sufficient inhomogeneity in these cases to prevent time−temperature-superposition of the measured flow curves. While all anionic polymerization-based tapered block copolymers could technically be considered a certain form of gradient copolymer, it was the development of controlled radical polymerization in the 1990s which led to the ability to controllably create purely interphase materials with extensive composition variation involving many comonomer combinations. In the absence of end block-driven behavior, it is now possible to study the purely interphase-driven thermal,[34,40–48] mechanical,[27,34,42,43] and ordering behavior[27,35,36,42,43,70] of such gradient copolymer materials.

Experimental Section

Copolymer Synthesis. The S/AS diblock copolymer (S-*block*-AS) was synthesized by sequential, batch nitroxide-mediated controlled radical polymerization (NM-CRP) with 2,2,5-trimethyl-3-(1-phenylethoxy)-4-phenyl-3-azahexane (A29)[31] as initiator. First, a polystyrene (PS) macroinitiator with M_n = 39 000 g/mol and M_w/M_n = 1.28 (by gel permeation chromatography (GPC)) was made using S (20 mL) and A29 (30 μL) at 115 °C for 2.5 h. Following reaction, the mixture was precipitated into excess methanol, and the resulting material was further washed via cycles of dissolution (tetrahydrofuran (THF)) and precipitation (methanol) before being dried under vacuum. This macroinitiator (0.748 g) was chain extended for 1.5 h at 100 °C with AS (11 mL) to yield a block copolymer with a cumulative S mole fraction, F_S, of 0.49 (^{1}H NMR) and M_n = 102 000 g/mol (calculated from the macroinitiator M_n and the F_S value). The S/AS random copolymer (S-*rand*-AS, F_S = 0.50, M_n = 106 000 g/mol) and the higher molecular weight gradient copolymer (S-*grad2*-AS, F_S = 0.56, M_n = 94 000 g/mol) are the same as in ref 34. The lower molecular weight gradient copolymer (S-*grad1*-AS) was synthesized using the same conditions as S-*grad2*-AS except using 50% more initiator (F_S = 0.64, M_n = 51 000 g/mol). In order to verify the formation of a composition gradient, aliquots (∼ 1 mL) of the reaction mixture were collected at different reaction times. All polymers were isolated and washed as described above. The M_n values for S-*rand*-AS, S-*grad1*-AS, and S-*grad2*-AS were measured by GPC relative to PS standards using THF as eluent.

The S/nBA diblock copolymer (S-*block*-nBA) was synthesized sequentially using the same PS macroinitiator as the S-*block*-AS sample. This macroinitiator (0.836 g) was chain extended for 2.5 h at 90 °C with nBA (10 mL) to yield a block copolymer with F_S = 0.70 and M_n = 60 000 g/mol (calculated from the macroinitiator M_n and the F_S value). The S/nBA random copolymer (S-*rand*-nBA) was synthesized by bulk copolymerization of S (6 mL) and nBA (17 mL) at 70 °C for 20 min (<5% conversion) using azobisisobutyronitrile (50 mg) as initiator; the resulting S-*rand*-nBA had F_S = 0.45 and M_n = 110 000 g/mol. The first S/nBA gradient copolymer (S-*grad1*-nBA) was synthesized using semibatch NM-CRP by the addition of nBA to a test tube of S (10 mL) and A29 (12 μL). The nBA monomer was added at increasing flow rates, starting at 2 mL/h for 3 h, increasing to 4 mL/h for 3 h and finally at 6 mL/h for 3 h to yield a material with having F_S = 0.60, M_n = 95 000 g/mol. The second S/nBA gradient copolymer (S-*grad2*-nBA) was synthesized using a lower initial concentration of initiator (10 μL in 10 mL) and slower initial addition of nBA for the first 3 h of the synthesis (1 mL/h). The remainder of the nBA was added at 4 mL/h for 3 h and 6 mL/h for 2 h to yield a material having F_S = 0.61, M_n = 152 000 g/mol. As above with the S/AS gradient copolymers, aliquots were taken to verify the formation of a gradient composition. All polymers were isolated and washed as described above. The M_n values for S-*rand*-nBA, S-*grad1*-nBA, and S-*grad2*-nBA were measured by GPC relative to PS standards using THF as eluent.

Thermal Characterization. Thermal characterization was carried out using a differential scanning calorimeter (DSC, Mettler-Toledo DSC 822e) following the methods used in ref 31.

Rheology. Samples were hot-pressed into disks and annealed for 2 h at ∼30 °C or more above their T_g endsets from DSC. Rheological characterization was carried out using a Rheometrics Scientific ARES controlled-strain rheometer with 2.5-cm parallel-plate geometry. Copolymers were subjected to strain sweeps to verify their linear region of strain response followed by frequency sweeps at increasing temperatures using a shear strain (γ) of 10%.

SAXS. The S/AS copolymer samples were hot-pressed into cylindrical plug-shapes and annealed at 200 °C for 2 h. Room-temperature, synchrotron-based SAXS was performed on beam line 5ID of the Advanced Photon Source, using 14 keV radiation and an 8.6 m sample−detector distance. Collected patterns were analyzed using the software program Fit2D.[80]

Shear Alignment. For shear alignment of S-*grad2*-AS in the ARES rheometer, the sample was subjected to a frequency sweep at low strain (γ = 10%), then 30 min of high amplitude oscillatory shear (γ = 100%, ω = 1 rad/s), followed by another frequency sweep at low strain. Experiments were performed at 200 °C.

For observation of shear alignment via SAXS, experiments were performed at 160 °C on beam line 5BM-D of the Advanced Photon Source, using 7 keV radiation, a 1.5 m sample−detector distance, and a rotating disk shear cell (Linkam CSS-450) customized for X-ray use,[81] which allows for examination in the flow-vorticity ("1−3") plane.

Results and Discussion

Characterization of Gradient Copolymers and Proof of Degree of Microphase Segregation. Figure 2 demonstrates the formation of composition gradients in the S/nBA and S/AS gradient copolymer samples through the evolution of the cumulative styrene mole fraction (F_S) with increasing apparent normalized chain length. The apparent normalized chain length was determined via the ratio of the M_n value for an aliquot

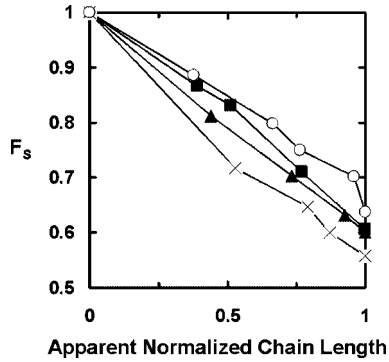

Figure 2. Cumulative styrene mole fraction (F_S) as a function of apparent normalized chain length for S-*grad1*-AS (open circles), S-*grad2*-AS (×), S-*grad1*-nBA (triangles), and S-*grad2*-nBA (squares).

Table 1. Molecular Characterization of S/AS and S/nBA Copolymers

sample	M_n (g/mol)	F_S
S-*block*-AS	102 000[a]	0.49
PS macroinitiator	39 000	1
S-*rand*-AS	106 000[b]	0.50
S-*grad1*-AS	51 000[b]	0.64
S-*grad2*-AS	94 000[b]	0.56
S-*block*-nBA	60 000[a]	0.70
PS macroinitiator	39 000	1
S-*rand*-nBA	110 000[b]	0.45
S-*grad1*-nBA	95 000[b]	0.60
S-*grad2*-nBA	152 000[b]	0.61

[a] M_n value was determined from the M_n of PS macroinitiator and the F_S value. [b] Characterized relative to PS standards by GPC with THF as eluent.

copolymer sample recovered at a given time during the polymerization relative to that obtained for the copolymer at the end of the polymerization. (Given that the aliquot sample and copolymer M_n values were determined by GPC relative to PS standards, the normalized chain length is only apparent and not absolute.) The comonomer compositions of all the gradient copolymer samples clearly change with increasing molecular weight to incorporate increasing amounts of nBA or AS as the chains grow, yielding similar final F_S values (F_S ranges from 0.56 to 0.64). A greater difference is seen between the two S/AS gradient composition curves than the S/nBA gradient composition curves, but it will be shown later that the lower χ value for the S/nBA system leads to greater sensitivity of S/nBA copolymer microphase segregation to gradient structure. The molecular characterization of the S/AS and S/nBA copolymers used in this study is summarized in Table 1.

The derivatives of the DSC enthalpy curves for the gradient copolymers are shown in Figure 3. This derivative technique has been used in studies of block copolymers,[39] polymer blends[39,82] and gradient copolymers[31,45,47] since it better demonstrates subtleties in thermal behavior than raw enthalpy curves. Our group has shown that this is a sensitive method for evaluating the relative degree of microphase segregation in gradient copolymers by allowing for easy comparison of T_g breadth, which corresponds to the range of compositions present.[31]

Figure 3a shows the derivative heat curves for the two S/AS gradient copolymer samples. The T_g breadth of S-*grad1*-AS spans the majority of the range of temperatures intermediate to the T_gs of its homopolymer components (polystyrene T_g = 100 °C, poly(4-acetoxystyrene) T_g = ~130 °C). This indicates that the material has microphase segregated into A-rich and B-rich regions with large composition variation. The derivative heat curve of S-*grad2*-AS is similar in shape and breadth to the

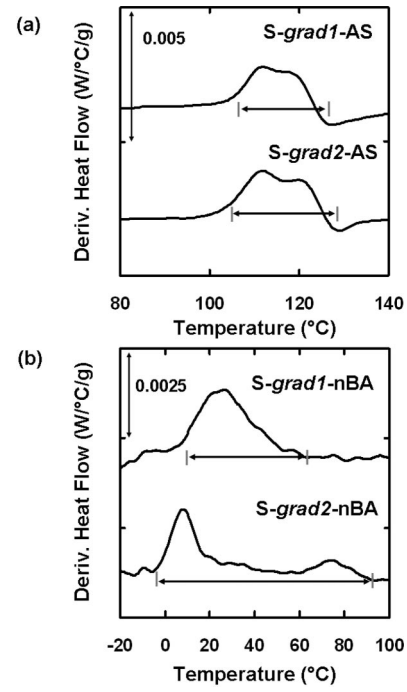

Figure 3. (a) Derivatives of DSC heating curves for S/AS gradient copolymers. (b) Derivatives of DSC heating curves for S/nBA gradient copolymers. Arrows indicate the breadth of T_g for respective samples.

S-*grad1*-AS sample, indicating a similar degree of microphase segregation despite the higher molecular weight of the sample. Their similarity in shape is consistent with their equivalent rates of monomer addition during synthesis, while their similarity in breadth is consistent with the relatively high Flory−Huggins parameter value of the S/AS system (we estimate χ to be ~0.45[83–85]). Using this value, we estimate $\chi N > 150$ for S-*grad1*-AS, which places even this lower molecular weight case in the strong segregation regime, corroborating our previous assessment of a composition profile with A-rich and B-rich regions.

Figure 3b shows the derivative heat curves for the S/nBA gradient copolymers. The T_g breadths of S-*grad1*-nBA and S-*grad2*-nBA are ~50 and ~90 °C, respectively. This indicates a significantly higher degree of microphase segregation in the latter case, consistent with higher molecular weight and more blocklike structure (from the slower initial addition of nBA during synthesis) of S-*grad2*-nBA. The sensitivity of the degree of S/nBA microphase segregation to molecular weight and chain design is due to the lower χ value of the S/nBA system (values reported for the S/nBA Flory–Huggins parameter are χ = 0.034[86] and χ = 0.087[87]) compared to the S/AS system. Using this value, we estimate χN = ~30–70 for S-*grad1*-nBA and χN = ~50–120 for S-*grad2*-nBA. This places S-*grad2*-nBA in the strong segregation regime, while S-*grad1*-nBA is intermediate to the weak and strong segregation regimes; this is consistent with the amount of microphase segregation that is apparent from calorimetry for each sample.

Rheology of S/AS Copolymers. Figure 4 shows the frequency dependence of the shear storage modulus (G'), shear loss modulus (G'') and phase angle (δ) for the S/AS copolymers at 200 °C. S-*rand*-AS resembles classic terminal or Newtonian behavior (i.e., $G' \sim \omega^2$ and $G'' \sim \omega$ as $\omega \rightarrow 0$) with a critical frequency (ω_c) at 8 rad/s, where G' crosses below G'', and δ passes through 45°. S-*block*-AS exhibits a similar crossover at higher frequencies (ω_c = 20 rad/s), but the moduli cross again at 0.1 rad/s to yield a second critical frequency (ω_{c2}), resulting in $G' > G''$ or solidlike behavior at low frequencies. Between

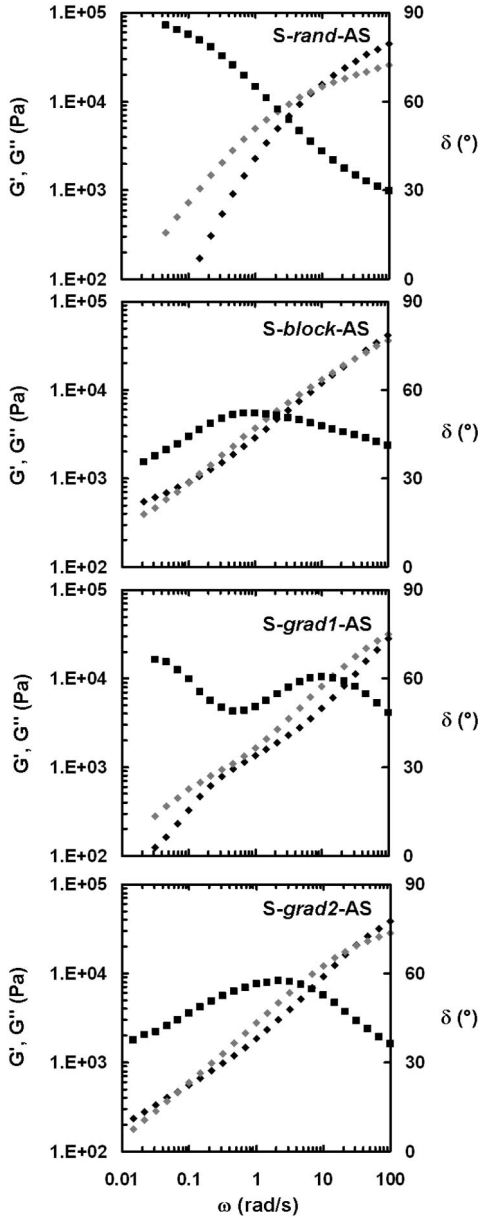

Figure 4. Frequency dependence of moduli G' (black diamonds), G'' (gray diamonds) and phase angle δ (squares) at 200 °C and a strain amplitude of 10% for S/AS copolymers.

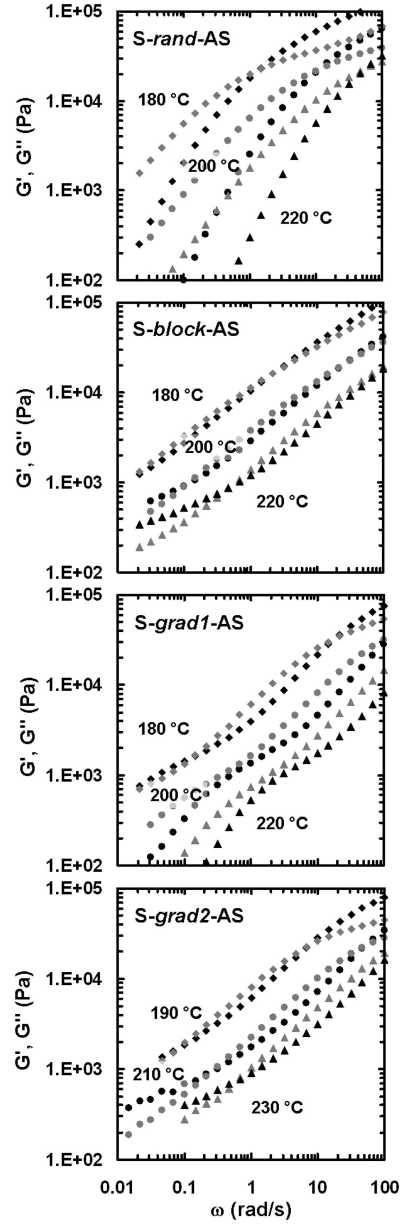

Figure 5. Frequency dependence of moduli G' (black symbols) and G'' (gray symbols) at various temperatures and a strain amplitude of 10% for S/AS copolymers.

these critical frequencies, G' and G'' enclose a lens-shaped region, and their greatest separation is reflected as a maximum in the phase angle ($\delta_{max} = 52°$). This low-frequency solidlike behavior is typical for ordered block copolymers[13–24] or networked materials[88] where structure interferes with large-scale relaxation. In S-*grad1*-AS, the higher frequency crossover is just outside the range of measured frequencies ($\omega_c > 100$ rad/s), but a similar lens-shaped region is seen to develop between $\omega = 100$ rad/s and $\omega = 0.5$ rad/s. At $\omega = 0.5$ rad/s, the curves converge but do not cross over and instead diverge again as ω decreases, and appear to decrease monotonically with frequency. These events are evident in the phase angle curve as a maximum ($\omega = 10$ rad/s) and then a minimum ($\omega = 0.5$ rad/s) as frequency decreases. This complexity in behavior indicates that there is some degree of microphase segregation for this sample; however, the higher values of δ at low frequencies suggest a lower degree of microphase segregation than in the S-*block*-AS sample and a trend toward terminal liquidlike relaxation at low frequencies. The final case, S-*grad2*-AS, exhibits curves similar in shape to those for S-*block*-AS but with greater separation of G' and G'' between the two critical frequencies ($\omega_c = 30$ rad/s and $\omega_{c2} = 0.07$ rad/s) and δ_{max} being higher at 57°. In this case, as in S-*block*-AS, the response is trending more solidlike at the lowest frequencies.

In Figure 5, the G' and G'' curves of the S/AS copolymers are shown for temperatures above and below 200 °C. For the random, block and S-*grad2*-AS cases, the curves appear merely shifted along the frequency axis as the temperature changes, indicating no change to the degree of ordering. However, with S-*grad1*-AS, G' appears to be shifting further below G'' at $\omega < \omega_c$, with multiple lower-frequency crossovers at 180 °C but none at higher temperatures. The moduli at these higher temperatures also decrease rapidly at the lowest measured frequencies, again resembling terminal behavior.

To compare more easily the temperature dependence of the viscoelastic behavior, we use van Gurp−Palmen plots[89,90] of δ as a function of complex modulus ($|G^*|$) (Figure 6). Where the time−temperature superposition (tTS) principle holds, curves

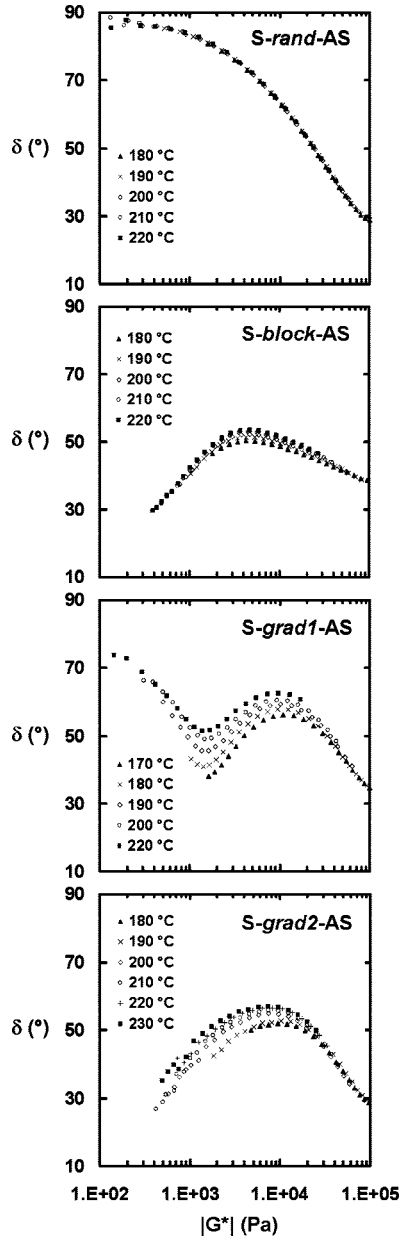

Figure 6. Van Gurp−Palmen plots for S/AS copolymers. (Note: $|G^*| = (G'^2 + G''^2)^{1/2}$.)

for different temperatures will overlap. However, when tTS does not hold (as generally to be expected in systems with phase segregation), this presentation facilitates comparison of data taken at different temperatures, free from any uncertainty associated with shifting curves along the frequency axis. Such plots have been applied in studies of polydispersity,[91] blend miscibility[90,92] and copolymers.[93]

In the van Gurp-Palmen plot for S-*rand*-AS, the curves overlap for the full range of $|G^*|$ measured, with δ approaching 90° at lower modulus values; this is consistent with behavior for a homogeneous material. In the S-*block*-AS case, the curves all exhibit maxima in δ, with clear superposition at higher and lower values of $|G^*|$ but less clean overlap at intermediate values. The slight shift in δ at these intermediate values is hypothesized to arise from gradual alignment of the block copolymer domains, since little change is seen at lower values of $|G^*|$ to indicate the system is becoming less ordered. At the intermediate and lower ranges of $|G^*|$, the two gradient copolymer cases show a more substantial increase in δ with increasing temperature. This is consistent with both materials becoming less microphase segregated at higher temperature and thus displaying more liquidlike behavior. This effect is especially strong with S-*grad1*-AS, where δ approaches 75° at lower $|G^*|$.

Thus, while the two gradient copolymers appear microphase segregated over a similar range of compositions in the T_g analysis, their rheological signatures reveal very different behavior arising from their difference in molecular weight. The higher molecular weight sample, S-*grad2*-AS, exhibits nonterminal behavior akin to that of the block copolymer, which suggests a similar level of ordering. However, an examination of the gradient copolymer curves in a van Gurp−Palmen plot reveals greater temperature dependence in behavior than the block case. This is consistent with the work of Lefebvre et al., which predicted that the composition amplitudes of the A-rich and B-rich regions change very gradually with χN.[36] S-*grad1*-AS exhibits more complicated behavior, with δ increasing rather than decreasing at the lowest values of $|G^*|$ (corresponding to the lowest frequencies). In the higher $|G^*|$ range (corresponding to the higher frequency range), S-*grad1*-AS exhibits higher local maximum δ values than S-*grad2*-AS; this suggests that S-*grad1*-AS is less microphase segregated than S-*grad2*-AS, consistent with its lower molecular weight.[94] Phase angle curves of similar shape to the S-*grad1*-AS case have previously been observed in a styrene/butadiene (S/B) block copolymer system with a random middle block,[95] which suggests that such behavior is consistent with interphase-containing systems. However, the S/B block systems demonstrate little temperature dependence, which may be due to the phase-stabilizing effects of the homopolymer end blocks.

Rheology of S/nBA Copolymers. Figure 7 shows the frequency dependence of G', G'', and δ for the S/nBA copolymers. Since the T_gs for the homopolymer cases are substantially further apart for the S/nBA system ($\Delta T_g = 155$ °C) than the S/AS system ($\Delta T_g = 30$ °C), the transition temperature to fully rubbery behavior for the S/nBA copolymers was widely variable. Thus, rather than presenting data at a single temperature for all the samples, a representative temperature was chosen which captured behavior near and below ω_c.

The S/nBA random case resembles classic terminal behavior while the S/nBA block case shows the same dual crossover behavior that was seen in the S/AS block case ($\omega_c = 30$ rad/s and $\omega_{c2} = 0.1$ rad/s). The S-*grad1*-nBA sample appears Newtonian, indicating that the system is at most weakly microphase segregated, consistent with the smaller T_g breadth of the sample as measured using calorimetry. The moduli curves for the S-*grad2*-nBA sample appear to be decreasing monotonically, but their power law dependences are far from Newtonian with $G' \sim \omega^{0.66}$ and $G'' \sim \omega^{0.58}$ as $\omega \rightarrow 0$. This is reflected in the phase angle, which exhibits a maximum $\delta_{max} = 61°$ as ω approaches lower values. The phase angle peak is much broader than the block case, appearing plateaulike as $\omega \rightarrow 0$. This suggests that S-*grad2*-nBA is not as highly microphase segregated as S-*block*-nBA or the S/AS gradient samples but that there is sufficient nanoheterogeneity to inhibit terminal behavior.

In Figure 8, G' and G'' curves are plotted for the S/nBA copolymers at temperatures above and below the representative temperatures in Figure 7. The random and block cases appear merely shifted along the frequency axis consistent with tTS, suggesting no phase change with temperature. For S-*grad1*-nBA, very subtle curvature is present in G' at low moduli values, suggesting that there may be some weak effects from heterogeneity. More substantial changes appear in the S-*grad2*-nBA case, as the slopes of G' and G'' below ω_c grow steeper and diverge more quickly with increasing temperature. An evaluation of the low-frequency power law dependences at 90 °C show $G' \sim \omega^{0.58}$ and $G'' \sim \omega^{0.55}$, while at 130 °C these have changed to $G' \sim \omega^{0.87}$ and $G'' \sim \omega^{0.75}$. This sample clearly shows a

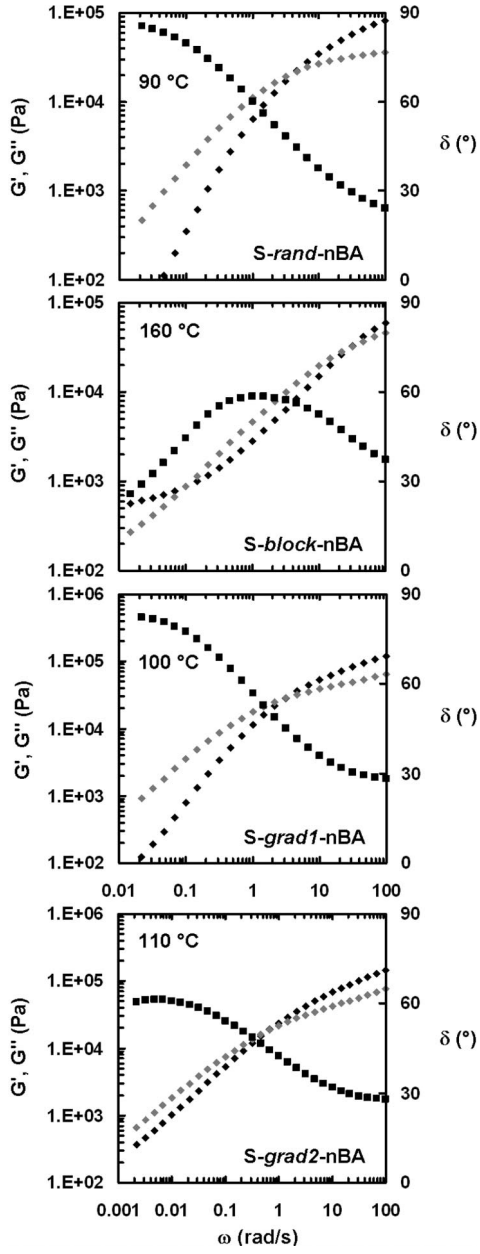

Figure 7. Frequency dependence of moduli G' (black diamonds), G'' (gray diamonds), and phase angle δ (squares) at a strain amplitude of 10% for S/nBA copolymers.

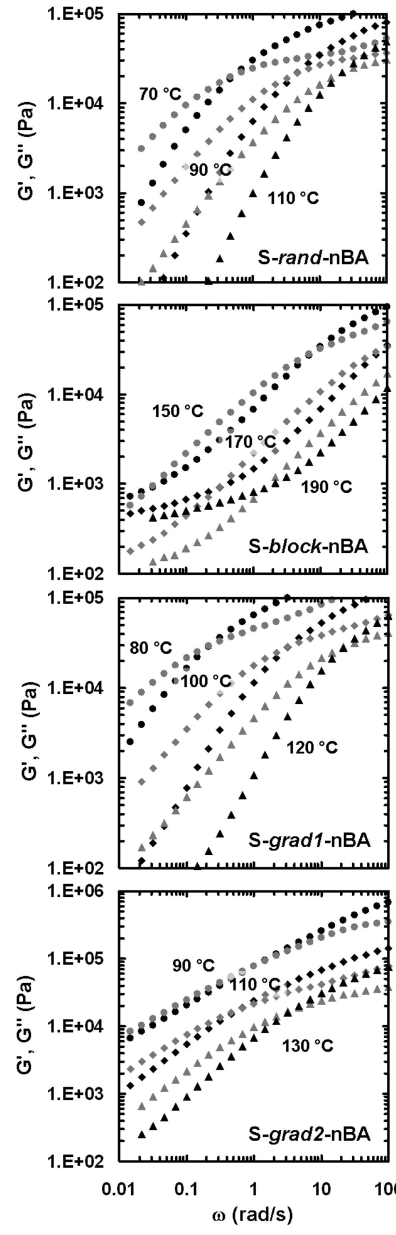

Figure 8. Frequency dependence of moduli G' (black symbols) and G'' (gray symbols) at various temperatures and a strain amplitude of 10% for S/nBA copolymers.

gradual evolution of behavior from that of a nanoheterogeneous system to that of a more homogeneous system with increasing temperature.

The data for the S/nBA copolymers at different temperatures are combined in van Gurp−Palmen plots for simple evaluation of temperature dependent changes in viscoelastic character (Figure 9). The random case appears essentially temperature independent, while the block and S-*grad1*-nBA cases overlap closely, but there is a subtle shift toward higher δ at intermediate values of $|G^*|$ with increasing temperature. In the block case, this may be due to gradual alignment of the system under the oscillatory shear, as in the S/AS block case. With S-*grad1*-nBA, we see that the behavior is not fully terminal, counter to what the curves at 100 °C in Figure 7 had suggested. At the highest temperatures, δ appears to be curving slightly downward at low $|G^*|$ rather than plateauing toward 90°, which suggests there may be some heterogeneity effects influencing the low frequency behavior of the material. The changes with S-*grad2*-nBA are the most dramatic; the behavior grows more liquidlike with increasing temperature, e.g., $\delta_{max} = 55°$ at 100 °C while $\delta_{max} = 75°$ at 180 °C. This indicates a gradual change in the degree of microphase segregation over the measured temperature range.

The rheological properties of the S/nBA gradient copolymer samples clearly reflect the difference in their degrees of microphase segregation as observed using DSC. For the less microphase segregated S-*grad1*-nBA, the behavior appears close to terminal, with some slight curvature visible at low frequencies that is suggestive of minor heterogeneity effects, such as composition fluctuations.[2] Such behavior indicates that over the range of temperatures studied, this material is either disordered or microphase segregated with a relatively small amplitude in its sinusoidal composition profile. A comparison of its T_g breadth (50 °C) against that of the homogeneous S-*rand*-nBA sample (20 °C (data not shown)) indicates that S-*grad1*-nBA is weakly microphase segregated rather than disordered. For the more highly microphase segregated S-*grad2*-nBA, the behavior changes from heterogeneous and solidlike toward homogeneous and liquidlike over a temperature range of 80 °C. This is reflective of the predictions by Lefebvre et al.[36] of slowly

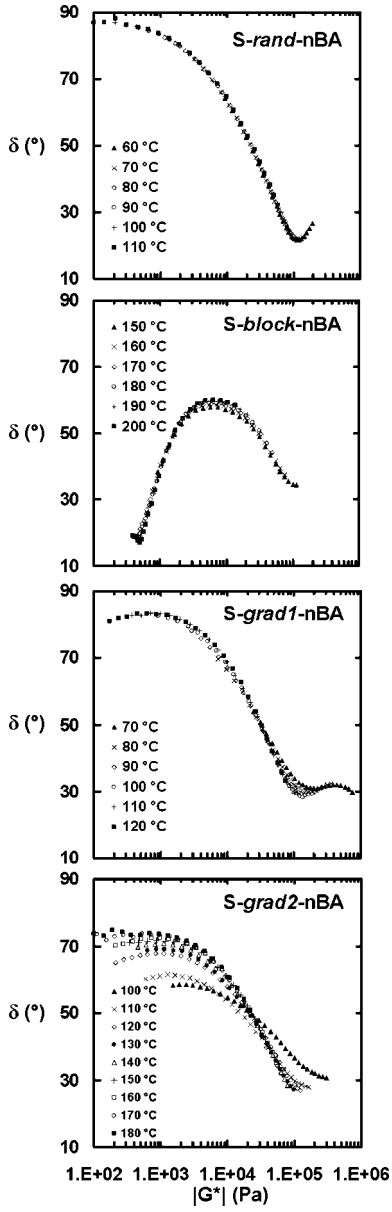

Figure 9. Van Gurp−Palmen plots for S/nBA copolymers. (Note: $|G^*| = (G'^2 + G''^2)^{1/2}$.)

changing composition amplitudes with χN for gradient copolymers. Thus, over the range of temperatures studied, this sample evolves from the weak segregation regime toward the disordered regime. It should also be noted that the S/nBA block copolymer exhibits behavior suggesting a much higher degree of microphase segregation and ordering than the two gradient cases, despite having a much lower molecular weight; this is reflective of the higher $(\chi N)_c$ that was predicted for gradient copolymers by Lefebvre et al.[36]

SAXS Analysis. To complement the results from rheology, SAXS was performed at room temperature on preannealed solid-state S/AS copolymers (Figure 10). The S-*block*-AS sample exhibits two SAXS peaks. (The two peaks appear at q ratios of 1:2, consistent with the lamellar ordering expected for a sample that is roughly symmetric in composition.) The two gradient cases each show a single scattering peak, providing direct evidence of microphase segregation. The S-*grad1*-AS peak is at $q = 0.14$ nm^{-1} corresponding to a d-spacing of 45 nm while the S-*grad2*-AS peak is at $q = 0.10$ nm^{-1} corresponding to a larger d-spacing of 63 nm; these values, which represent the periodicity of the domains, are consistent with the relative

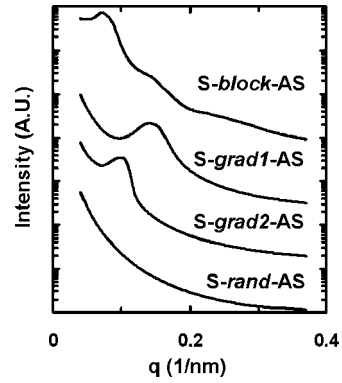

Figure 10. Small-angle X-ray scattering of solid S/AS copolymers at room temperature. Curves have been shifted vertically for clarity.

molecular weights of the samples.[96] The peak breadth and lack of higher order reflections may suggest limited long-range order; however, it should be noted that a symmetric lamellar nanophase structure with a sinusoidal composition profile, as predicted in the calculations of Lefebvre et al.,[36] would fail to exhibit higher order reflections.[97] There also exists the possibility that a potential second peak is suppressed by extinction nodes that occur in ordered block copolymer structures with symmetric domain volume fractions;[98] since the degree of comonomer mixing within the gradient copolymer domains is unknown, it is not possible to calculate the actual volume fractions. No peak is observed for S-*rand*-AS, as expected for a homogeneous material.

The 2-D SAXS patterns of the solid S-*block*-AS and S-*grad2*-AS samples were highly anisotropic (data not shown), suggesting flow-induced alignment of microphase separated structures that was unable to relax during the subsequent annealing (the following section reports a limited study of shear alignment in S-*grad2*-AS). Conversely, the 2-D SAXS pattern for the annealed S-*grad1*-AS sample was isotropic. This is consistent with our earlier observation of liquidlike low frequency response in the melt rheology of S-*grad1*-AS, in contrast to the highly elastic behavior of the other two microphase separated samples.

Shear Alignment of Gradient Copolymers. Given the sinusoidal nature of the gradient copolymer composition profiles, it is of interest to study whether these fully interphase materials are able to undergo shear alignment similar to that of block copolymers. To this end, limited studies were carried out on S-*grad2*-AS using a combination of rheology and SAXS.

Figure 11 compares G', G'', and δ curves for S-*grad2*-AS before and after shear alignment. With shear alignment, G' and G'' decrease by factors of ~2 to 5, and the region enclosed by the G' and G'' curves between the critical frequencies increases in area. There is also a shift and broadening of the δ peak as the sample is rendered more liquidlike as a result of large-amplitude shearing ($\delta_{max} = 57°$ before shear, $\delta_{max} = 71°$ after shear). These behaviors are in accordance with shear alignment studies of block copolymers.[13,15,18] (Our S-*block*-AS sample was subjected to the same regimen of oscillatory shear and demonstrated similar manifestations of shear alignment, as expected (data not shown).)

As shown in Figure 12, *in situ* SAXS during steady shearing of melt-state S-*grad2*-AS confirms the ability of flow to induce significant alignment of ordered gradient copolymer nanostructures. In the as-loaded state prior to shear, only weak, isotropic scattering is observed (Figure 12a). After inception of shear flow at 0.1 s^{-1}, a scattering peak at the expected q-value emerges and concentrates along the vorticity axis of the shear flow (Figure 12b). While SAXS data are insufficient to determine the microphase segregated morphology, this scattering pattern

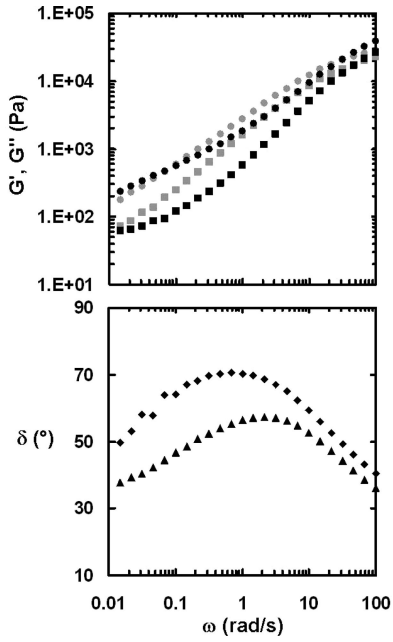

Figure 11. Frequency dependence before and after high amplitude shear of G' (before - black circles, after - black squares), G'' (before - gray circles, after - gray squares), and phase angle (before - triangles, after - diamonds) for S-*grad2*-AS copolymer at 200 °C under a strain amplitude of 10%. (Shear alignment was performed for 30 min at a frequency of 1 rad/s and a strain of 100%.)

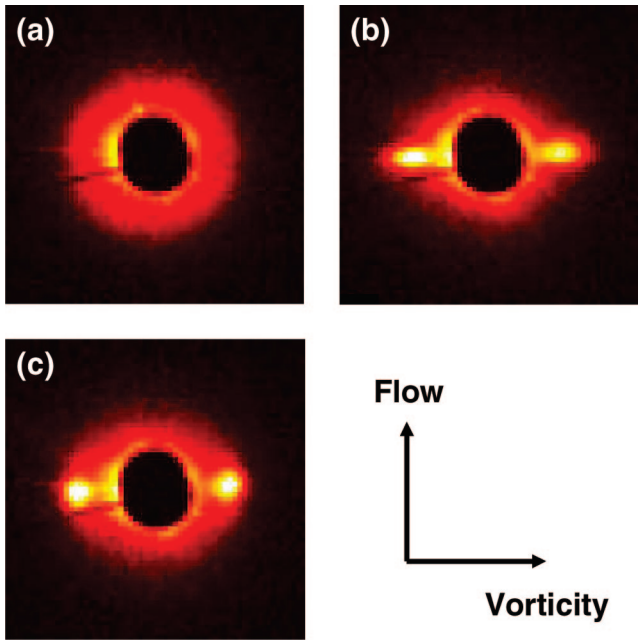

Figure 12. 2-D SAXS images of S-*grad2*-AS copolymer melt during and following flow alignment during steady shear at a rate of 0.1 s^{-1}. Images were collected (a) following sample loading and prior to shear flow, (b) after 1290 s of shearing, just prior to flow cessation, and (c) after 1080 s of relaxation. $T = 160$ °C.

resembles that found with alignment of a lamellar phase in the "perpendicular" orientation, with layer normals along the vorticity axis.[17] (With only data from the flow-vorticity plane available in this limited study, we cannot more fully assess the 3-D alignment state generated by shear flow.) Following cessation of shear flow, only modest relaxation of the shear-induced anisotropy is observed (Figure 12c). Thus, shear flow is capable of inducing profound changes in gradient copolymer structure that presumably underlie the rheological changes in Figure 11 and that relax very slowly upon flow cessation. After 20 min of relaxation, the sample in Figure 12c was sheared again at a higher rate, 0.5 s^{-1}. The higher shear rate scattering pattern exhibits significant anisotropy with the same perpendicular character found at 0.1 s^{-1} and, as in Figure 12c, does not exhibit significant relaxation (data not shown).

Conclusion

Gradient copolymers of S/AS, a strongly segregating comonomer system, and S/nBA, a weakly segregating comonomer system, were synthesized by controlled radical polymerization and studied using low-amplitude oscillatory shear over a range of temperatures. Comparisons were made to S/AS and S/nBA random and block copolymers. The S/AS gradient copolymers demonstrated a higher degree of microphase segregation, with rheological behavior resembling that of the block copolymer in the higher molecular weight case, and complicated but more liquidlike behavior in the lower molecular weight case. A lower degree of microphase segregation was observed in the S/nBA gradient copolymers, with the lower molecular weight sample exhibiting near terminal behavior, indicative of a weakly microphase segregated system, and the higher molecular weight, steeper gradient sample exhibiting behavior evolving from solidlike to liquidlike over 80 °C. All gradient copolymers besides the one exhibiting near-terminal properties showed temperature-dependent behavior over extended temperature ranges, supporting the predictions of Lefebvre et al.[36] that gradient copolymers exhibit a more gradual change in composition amplitude with respect to χN than block copolymers. Analysis using SAXS was also carried out on the S/AS copolymers. Multiple SAXS peaks were seen in the block case while single strong peaks were seen in the gradient cases, consistent with the observation of microphase segregation by rheology. Studies by SAXS and rheology demonstrated that shear alignment is possible in gradient copolymers, despite the gradually varying composition profiles of these architectures. These findings make clear the significant roles of segregation strength, molecular weight, sequence distribution along the chain backbone, and temperature in gradient copolymer nanophase separation. Greater understanding of such behavior is important for potential applications of gradient copolymers as damping materials.

Acknowledgment. This work was funded by Northwestern University and the NSF-MRSEC program (Grant DMR-0520513) at the Materials Research Center of Northwestern University. Portions of this work were performed at the DuPont-Northwestern-Dow Collaborative Access Team (DND-CAT) located at Sector 5 of the Advanced Photon Source (APS). We thank the staff of DND-CAT for their help with setup of SAXS experiments and the Polymer Group from the University of Minnesota for donating some of their beamline time at the APS. DND-CAT is supported by the E.I. DuPont Nemours and Co., the Dow Chemical Company, the National Science Foundation through Grant DMR-9304725 and the State of Illinois through the Department of Commerce and the Board of Higher Education Grant IBHE HECA NWU 96. Use of the APS was supported by the U.S. Department of Energy, Office of Science, Office of Basic Energy Sciences, under Contract No. DE-AC02-06CH11357 and the U.S. Department of Energy, Basic Energy Sciences, Office of Research Safety, under Contract No. W-31-102-Eng-38.

References and Notes

(1) Leibler, L. *Macromolecules* **1980**, *13*, 1602–1617.
(2) Fredrickson, G. H.; Helfand, E. *J. Chem. Phys.* **1987**, *87*, 697–705.
(3) Bates, F. S. *Science* **1991**, *251*, 898–905.

(4) The term "tapered block copolymer(s)" appeared in the following patents from The Netherlands and Japan during the period **1968**−**1975**: *Copolymers of conjugated dienes and styrene*. Neth. Appl. NL 6616691, May 29, **1968**. Nishikawa, T.; Kawaharada, S.; Asai S.; Saito, C. *Adhesive compositions.* Jpn. Kokai Tokkyo Koho JP 49092162 19740903, **1974**. Horiie, S.; Asai, S.; Moriya, Y. *Tapered block copolymers.* Jpn. Kokai Tokkyo Koho JP 501398890 19751108, **1975**.

(5) Cunningham, R. E. *J. Appl. Polym. Sci.* **1978**, *22*, 2907–2913.

(6) Tsukahara, Y.; Nakamura, N.; Hashimoto, T.; Kawai, H.; Nagaya, T.; Sugimura, Y.; Tsuge, S. *Polym. J.* **1980**, *12*, 455–466.

(7) Hashimoto, T.; Tsukahara, Y.; Tachi, K.; Kawai, H. *Macromolecules* **1983**, *16*, 648–657.

(8) Hashimoto, T.; Tsukahara, Y.; Kawai, H. *Polym. J.* **1983**, *15*, 699–711.

(9) Creutz, S.; Jérôme, R.; Kaptijn, G. M. P.; van der Werf, A. W.; Akkerman, J. M. *J. Coat. Tech.* **1998**, *70*, 41–46.

(10) The term "graded block copolymer" appeared in the following patents in the early 1970's: *Polystyrene block copolymers.* Fr. Demande FR21815128, December 3, **1973**. Durst, R. R. *High impact two-component polystyrene blends.* U.S. Patent 3,907,931, September 23, **1975**. Durst, R. R. *Polystyrene-graded block copolymer blends.* Br. Patent PI 1389911, April 9, **1975**.

(11) Aggarwal, S. L. *Polymer* **1976**, *17*, 938–956.

(12) Morales, G.; de Leon, R. D.; Acuna, P.; Flores, R. F.; Robles, A. M. *Polym. Eng. Sci.* **2006**, *46*, 1333–1341.

(13) Larson, R. G. In *The Structure and Rheology of Complex Fluids*. Oxford University Press: New York, 1998; Chapter 13, pp 607−629.

(14) Morrison, F.; LeBourvellec, G.; Winter, H. H. *J. Appl. Polym. Sci.* **1987**, *33*, 1585–1600.

(15) Riise, B. L.; Fredrickson, G. H.; Larson, R. G.; Pearson, D. S. *Macromolecules* **1995**, *28*, 7653–7659.

(16) Winey, K. I.; Patel, S. S.; Larson, R. G.; Watanabe, H. *Macromolecules* **1993**, *26*, 2542–2549.

(17) Pinheiro, B. S.; Winey, K. I. *Macromolecules* **1998**, *31*, 4447–4456.

(18) Larson, R. G.; Winey, K. I.; Patel, S. S.; Watanabe, H.; Bruinsma, R. *Rheol. Acta* **1993**, *32*, 245–253.

(19) Sakamoto, N.; Hashimoto, T.; Han, C. D.; Kim, D.; Vaidya, N. Y. *Macromolecules* **1997**, *30*, 1621–1632.

(20) Han, C. D.; Kim, J.; Kim, J. K. *Macromolecules* **1989**, *22*, 383–394.

(21) Mai, S.-M.; Mingvanish, W.; Turner, S. C.; Chaibundit, C.; Fairclough, J. P. A.; Heatley, F.; Matsen, M. W.; Ryan, A. J.; Booth, C. *Macromolecules* **2000**, *33*, 5124–5130.

(22) Almdal, K.; Mortensen, K.; Ryan, A. J.; Bates, F. S. *Macromolecules* **1996**, *29*, 5940–5947.

(23) Morkved, T. L.; Lu, M.; Urbas, A. M.; Ehrichs, E. E.; Jaeger, H. M.; Mansky, P.; Russell, T. P. *Science* **1996**, *273*, 931–933.

(24) Marencic, A. P.; Wu, M. W.; Register, R. A.; Chaikin, P. M. *Macromolecules* **2007**, *40*, 7299–7305.

(25) Pakula, T.; Matyjaszewski, K. *Macromol. Theory Simul.* **1996**, *5*, 987–1006.

(26) While the term "gradient copolymer" first appeared in a 1977 patent (Bailey, F. E.; Von Dohlen, W. C.; Matzner, M.; Young, R. H.; Robeson, L. M. *Gradient polymers of two or more α-mono-olefinic monomers capable of polymerizing with themselves and each other*. U.S. Patent 4,065,520, December 27, **1977**) related to a gaseous-state copolymerization, according to SciFinder Scholar, it did not reappear in the peer-reviewed or patent literature until 1996 with the publication of ref 25.

(27) Matyjaszewski, K.; Ziegler, M. J.; Arehart, S. V.; Greszta, D.; Pakula, T. *J. Phys. Org. Chem.* **2000**, *13*, 775–786.

(28) Matyjaszewski, K.; Xia, J. H. *Chem. Rev.* **2001**, *101*, 2921–2990.

(29) Kryszewski, M. *Polym. Adv. Technol.* **1998**, *9*, 244–259.

(30) Kim, J.; Gray, M. K.; Zhou, H. Y.; Nguyen, S. T.; Torkelson, J. M. *Macromolecules* **2005**, *38*, 1037–1040.

(31) Kim, J.; Mok, M. M.; Sandoval, R. W.; Woo, D. J.; Torkelson, J. M. *Macromolecules* **2006**, *39*, 6152–6160.

(32) Tao, Y.; Kim, J.; Torkelson, J. M. *Polymer* **2006**, *47*, 6773–6781.

(33) Lefay, C.; Charleux, B.; Save, M.; Chassenieux, C.; Guerret, O.; Magnet, S. *Polymer* **2006**, *47*, 1935–1945.

(34) Mok, M. M.; Kim, J.; Torkelson, J. M. *J. Polym. Sci., Part B: Polym. Phys.* **2008**, *46*, 48–58.

(35) Aksimentiev, A.; Holyst, R. *J. Chem. Phys.* **1999**, *111*, 2329–2339.

(36) Lefebvre, M. D.; de la Cruz, M. O.; Shull, K. R. *Macromolecules* **2004**, *37*, 1118–1123.

(37) Bates, F. S.; Rosedale, J. H.; Fredrickson, G. H. *J. Chem. Phys.* **1990**, *92*, 6255–6270.

(38) Rosedale, J. H.; Bates, F. S. *Macromolecules* **1990**, *23*, 2329–2338.

(39) Miwa, Y.; Usami, K.; Yamamoto, K.; Sakaguchi, M.; Sakai, M.; Shimada, S. *Macromolecules* **2005**, *38*, 2355–2361.

(40) Buzin, A. I.; Pyda, M.; Costanzo, P.; Matyjaszewski, K.; Wunderlich, B. *Polymer* **2002**, *43*, 5563–5569.

(41) París, R.; De la Fuente, J. L. *J. Polym. Sci., Part B: Polym. Phys.* **2007**, *45*, 1845–1855.

(42) Karaky, K.; Péré, E.; Pouchan, C.; Desbrières, J.; Dérail, C.; Billon, L. *Soft Matter* **2006**, *2*, 770–778.

(43) Karaky, K.; Billon, L.; Pouchan, C.; Desbrières, J. *Macromolecules* **2007**, *40*, 458–464.

(44) Gray, M. K.; Zhou, H. Y.; Nguyen, S. T.; Torkelson, J. M. *Macromolecules* **2004**, *37*, 5586–5595.

(45) Wong, C. L. H.; Kim, J.; Torkelson, J. M. *J. Polym. Sci., Part B: Polym. Phys.* **2007**, *45*, 2842–2849.

(46) Jakubowski, W.; Juhari, A.; Best, A.; Koynov, K.; Pakula, T.; Matyjaszewski, K. *Polymer* **2008**, *49*, 1567–1578.

(47) Kim, J; Torkelson, J. M. *Polym. Prepr.* **2007**, *48*, 221–222.

(48) Kraus, G.; Childers, C. W.; Gruver, J. T. *J. Appl. Polym. Sci.* **1967**, *11*, 1581–1591.

(49) Kraus, G.; Rollmann, K. W. *Angew. Makromol. Chem.* **1971**, *16/17*, 271–296.

(50) The samples provided to Hashimoto et al. (see ref 7) were reportedly from the group of Dr. G. Kraus from Phillips Petroleum Co., synthesized after methods described in the patent literature by Zelinski.

(51) Recently published data (Wong, C. L. H.; Kim, J.; Roth, C. B.; Torkelson, J. M. *Macromolecules* **2007**, *40*, 5631–5633.) of S/methyl methacrylate (MMA) copolymer systems show that gradient copolymers can undergo micellization in melt-state poly(methyl methacrylate) and exhibit larger critical micelle concentrations than analogous S/MMA block copolymers, indicating a lower degree of segregation strength.

(52) Karaky, K.; Clisson, G.; Reiter, G.; Billon, L. *Macrom. Chem. Phys.* **2008**, *209*, 715–722.

(53) Smith, A. P.; Douglas, J. F.; Amis, E. J.; Karim, A. *Langmuir* **2007**, *23*, 12380–12387.

(54) Hawker, C. J.; Bosman, A. W.; Harth, E. *Chem. Rev.* **2001**, *101*, 3661–3688.

(55) Gray, M. K.; Zhou, H. Y.; Nguyen, S. T.; Torkelson, J. M. *Macromolecules* **2003**, *36*, 5792–5797.

(56) Sardelis, K.; Michels, H. J.; Allen, G. *Polymer* **1984**, *25*, 1011–1019.

(57) Hodrokoukes, P.; Floudas, G.; Pispas, S.; Hadjichristidis, N. *Macromolecules* **2001**, *34*, 650–657.

(58) Kuntz, I. *J. Polym. Sci.* **1961**, *54*, 569.

(59) Chang, C. C.; Halasa, A. F.; Miller, J. W.; Hsu, W. L. *Polym. Int.* **1994**, *33*, 151–159.

(60) Annighofer, F.; Gronski, W. *Colloid Polym. Sci.* **1983**, *261*, 15–25.

(61) Annighofer, F.; Gronski, W. *Makromol. Chem.* **1984**, *185*, 2213–2231.

(62) Zielinski, J. M.; Spontak, R. J. *Macromolecules* **1992**, *25*, 5957–5964.

(63) Laurer, J. H.; Smith, S. D.; Samseth, J.; Mortensen, K.; Spontak, R. J. *Macromolecules* **1998**, *31*, 4975–4985.

(64) Knoll, K.; Niessner, N. *Macromol. Symp.* **1998**, *132*, 231–243.

(65) Adhikari, R.; Godehardt, R.; Lebek, W.; Weidisch, R.; Michler, G. H.; Knoll, K. *J. Macromol. Sci. Phys.* **2001**, *40*, 833–847.

(66) Huy, T. A.; Hai, L. H.; Adhikari, R.; Weidisch, R.; Michler, G. H.; Knoll, K. *Polymer* **2003**, *44*, 1237–1245.

(67) Jouenne, S.; González-Léon, J. A.; Ruzette, A.-V.; Lodefier, P.; Tencé-Girault, S.; Leibler, L. *Macromolecules* **2007**, *40*, 2432–2442.

(68) Wang, J.-S.; Greszta, D.; Matyjaszewski, K. *PMSE Prepr.* **1995**, *73*, 416–417.

(69) Dettmer, C. M.; Gray, M. K.; Torkelson, J. M.; Nguyen, S. T. *Macromolecules* **2004**, *37*, 5504–5512.

(70) Okabe, S.; Seno, K; Kanaoka, S.; Aoshima, S.; Shibayama, M. *Macromolecules* **2006**, *39*, 1592–1597.

(71) Bonne, T. B.; Ludtke, K.; Jordan, R.; Papadakis, C. M. *Macromol. Chem. Phys.* **2007**, *208*, 1402–1408.

(72) Sun, X. Y.; Luo, Y. W.; Wang, R.; Li, B. G.; Zhu, S. P. *AIChE J.* **2008**, *54*, 1073–1087.

(73) Phan, T. N. T.; Maiez-Tribut, S.; Pascault, J. P.; Bonnet, A.; Gerard, P.; Guerret, O.; Bertin, D. *Macromolecules* **2007**, *40*, 4516–4523.

(74) Ritz, P.; Latalova, P.; Kriz, J.; Genzer, J.; Vlcek, P. *J. Polym Sci., Part A: Polym. Chem.* **2008**, *46*, 1919–1923.

(75) Hoogenboom, R.; Fijten, M. W. M.; Wijnans, S.; van den Berg, A. M. J.; Thijs, H. M. L.; Schubert, U. S. *J. Comb. Chem.* **2006**, *8*, 145–148.

(76) Gray, M. K.; Zhou, H. Y.; Nguyen, S. T.; Torkelson, J. M. *Polymer* **2004**, *45*, 4777–4786.

(77) Vidts, K. R. M.; Dervaux, B.; Du Prez, F. E. *Polymer* **2006**, *47*, 6028–6037.

(78) Kim, J.; Sandoval, R. W.; Dettmer, C. M.; Nguyen, S. T.; Torkelson, J. M. *Polymer* **2008**, *49*, 2686–2697.

(79) Woo, D.; Kim, J.; Suh, M. H.; Zhou, H. Y.; Nguyen, S. T.; Lee, S. H.; Torkelson, J. M. *Polymer* **2006**, *47*, 3287–3291.

(80) Hammersley, A. P. ESRF. http://www.esrf.fr/computing/scientific/FIT2D (accessed Apr **2005**).

(81) Ugaz, V. M.; Burghardt, W. R. *Macromolecules* **1998**, *31*, 8474–8484.

(82) Song, M.; Hammiche, A.; Pollock, H. M.; Hourston, D. J.; Reading, M. *Polymer* **1995**, *36*, 3313–3316.
(83) The Flory−Huggins parameter for S/AS was calculated from group molar attraction constants after the methods of ref 84 applied to polymer systems based on theory from ref 85. A concise summary of these methods can be found in the following text: Rudin, A. In *The Elements of Polymer Science and Engineering*, 2nd ed.; Academic Press: San Diego, CA, 1999; pp. 447−458.
(84) Small, P. A. *J. Appl. Chem.* **1953**, *3*, 71.
(85) Huggins, M. L. *J. Chem. Phys.* **1941**, *9*, 440. Flory, P. J. *J. Chem. Phys.* **1941**, *9*, 660–661.
(86) Nicolas, J.; Ruzette, A. V.; Farcet, C.; Gérard, P.; Magnet, S.; Charleux, B. *Macromolecules* **2007**, *48*, 7029–7040.
(87) Rana, D.; Bag, K.; Bhattacharyya, S. N.; Mandal, B. M. *J. Polym. Sci., Part B: Polym. Phys.* **2000**, *38*, 369–375.
(88) Du, F. M.; Scogna, R. C.; Zhou, W.; Brand, S.; Fischer, J. E.; Winey, K. I. *Macromolecules* **2004**, *37*, 9048–9055.
(89) Dealy, J. M.; Larson, R. G. In *Structure and Rheology of Molten Polymers*. Hanser Gardner Publications: Cincinnati, OH, 2006; Chapter 5, pp 182−183.
(90) van Gurp, M.; Palmen, J. *Rheol. Bull.* **1998**, *67*, 5–8.
(91) Trinkle, S.; Friedrich, C. *Rheol. Acta* **2001**, *40*, 322–328.
(92) Li, R. M.; Yu, W.; Zhou, C. X. *J. Macromol. Sci., Part B: Phys.* **2006**, *45*, 889–898.
(93) de la Fuente, J. L.; Fernández-Garciá, M.; Cerrada, M. L.; Spiess, H. W.; Wilhelm, M. *Polymer* **2006**, *47*, 1487–1495.
(94) The increase in phase angle at low frequencies for S-*grad1*-AS (see Figure 6) hints at terminal liquidlike relaxation, although because of torque sensitivity limitations it was impossible to extend measurements to lower frequencies to determine whether δ would eventually approach 90°. One possible, speculative interpretation would be that while both gradient copolymer samples exhibit microphase separation at a local level, only the higher molecular weight S-*grad2*-AS sample exhibits the long-range ordering believed to be necessary to support the low frequency elastic response associated with lamellar systems.
(95) Thunga, M.; Staudinger, U.; Satapathy, B. K.; Weidisch, R.; Abdel-Goad, M.; Janke, A.; Knoll, K. *J. Polym. Sci., Part B: Polym. Phys.* **2006**, *44*, 2776–2788.
(96) While it is impossible to make a quantitative comparison of *d*-spacings involving gradient copolymers with differing comonomers and gradient architectures, it is interesting to note that the 28.6 nm *d*-spacing reported by Karaky et al. in ref[42] for a S/nBA gradient copolymer with apparent M_n = 51 800 g/mol is at least qualitatively consistent with the *d*-spacings of 45 and 63 nm reported here for the S-grad-AS gradient copolymers with apparent M_n values of 95 000 g/mol and 152 000 g/mol, respectively. In the future, we intend to do SAXS analysis of a broad array of gradient copolymers, including S/nBA systems.
(97) The reciprocal space construction of a sinusoidal pattern with periodicity *A* is delta functions at $\pm 2\pi/A$.
(98) Epps, T. H.; Cochran, E. W.; Bailey, T. S.; Waletzko, R. S.; Hardy, C. M.; Bates, F. S. *Macromolecules* **2004**, *37*, 8325–8341.

MA8009454